The *Plasmodium* rhoptry associated protein complex is important for parasitophorous vacuole membrane structure and intraerythrocytic parasite growth

Sreejoyee Ghosh[1], Kit Kennedy[2], Paul Sanders[3], Kathryn Matthews[1], Stuart A. Ralph[2], Natalie A. Counihan[1] and Tania F. de Koning-Ward[1]*

[1]School of Medicine, Deakin University, Waurn Ponds, Victoria, 3216, Australia

[2]Department of Biochemistry and Molecular Biology, Bio21 Molecular Science and Biotechnology Institute, Melbourne, Victoria, Australia

[3]The Burnet Institute, Melbourne, Victoria, Australia

Key words: *Plasmodium*, rhoptry, RAP, parasitophorous vacuole, host cell remodelling

Running title: Characterisation of the *Plasmodium* RAP complex

*To whom correspondence should be addressed:

Professor Tania de Koning-Ward

School of Medicine, Deakin University

Waurn Ponds, Victoria, 3217, Australia

Email: taniad@deakin.edu.au

Ph: +61-3 5227 2923, Fax: +61-3 5227 2615

This is the author manuscript accepted for publication and has undergone full peer review but has not been through the copyediting, typesetting, pagination and proofreading process, which may lead to differences between this version and the Version of Record. Please cite this article as doi: 10.1111/cmi.12733

ABSTRACT

Plasmodium parasites must invade erythrocytes in order to cause the disease malaria. The invasion process involves the coordinated secretion of parasite proteins from apical organelles that include the rhoptries. The rhoptry is comprised of two compartments, the neck and the bulb. Rhoptry neck proteins are involved in host cell adhesion and formation of the tight junction that forms between the invading parasite and erythrocyte, whereas the role of rhoptry bulb proteins remains ill-defined due to the lack of functional studies. In this study, we show that the rhoptry associated protein (RAP) complex is not required for rhoptry morphology or erythrocyte invasion. Instead, post-invasion when the parasite is bounded by a parasitophorous vacuolar membrane (PVM), the RAP complex facilitates the survival of the parasite in its new intracellular environment. Consequently, conditional knockdown of members of the RAP complex leads to altered PVM structure, delayed intra-erythrocytic growth and reduced parasitaemias in infected mice. This study provides evidence that rhoptry bulb proteins localising to the parasite-host cell interface are not simply by-products of the invasion process but contribute to the growth of *Plasmodium in vivo.*

Introduction

Malaria is an infectious disease of global significance, caused by protozoan parasites of the genus *Plasmodium*. In order to propagate and survive, *Plasmodium* parasites invade and then remodel host erythrocytes using specialised invasion and protein export machineries (reviewed in (de Koning-Ward *et al.*, 2016; Weiss *et al.*, 2016). The invasion of host erythrocytes involves a complex multi-step process that includes initial attachment of the parasite to the host cell, which is a reversible process, followed by reorientation of the parasite to juxtapose its apical end to the host cell. Irreversible attachment and formation of a tight junction with the host cell promptly ensues, with the parasite's actin-myosin motor powering its passage through this junction into the erythrocyte. Upon invasion, the parasite is surrounded by a parasitophorous vacuole (PV) that is bounded by a membrane termed the parasitophorous vacuole membrane (PVM). At distinct stages of the invasion process, parasite proteins and lipids are released from organelles located at the apical end of the parasite (the micronemes, rhoptries and dense granules) (Riglar *et al.*, 2011) but only in recent times have the molecular events that govern erythrocyte invasion begun to be resolved (Weiss *et al.*, 2016).

Of the apical organelles, the rhoptries are the most prominent. These organelles are large membrane-bound structures with a distinctive neck and bulb region (Bannister *et al.*, 2000) - despite no obvious physical separation between the two regions, each harbours diverse and distinct protein components that act at different stages of the invasion process (Counihan *et al.*, 2013). More than 30 proteins have been assigned as rhoptry proteins in the human malaria parasite, *P. falciparum* (Sam-Yellowe *et al.*, 2004; Kats *et al.*, 2006;

Counihan *et al.*, 2013) and proteomic analysis in the rodent malaria species *Plasmodium yoelii* has added a further 27 putative rhoptry proteins (Sam-Yellowe *et al.*, 2008). Proteins secreted from the rhoptry neck in *P. falciparum,* such as Rh1, 2a, 2b, 4 and 5, serve as adhesins that bind to host cell receptors (Rayner *et al.*, 2000; Rayner *et al.*, 2001; Triglia *et al.*, 2001; Kaneko *et al.*, 2002; Duraisingh *et al.*, 2003; Hayton *et al.*, 2008; Triglia *et al.*, 2009). Others, such as the rhoptry neck proteins (RON2, 4 and 5), are involved in formation of the tight junction in combination with secreted micronemal proteins (Alexander *et al.*, 2005; Cao *et al.*, 2009; Richard *et al.*, 2010; Lamarque *et al.*, 2011). Some of the *Plasmodium* rhoptry neck proteins have homologues in other apicomplexan parasites such as *Toxoplasma* and *Eimeria* (Bradley *et al.*, 2005; Proellocks *et al.*, 2010; Oakes *et al.*, 2013). The *Plasmodium* rhoptry bulb proteins (ROPs), however, lack homologues in other apicomplexan species. Many of the ROPs in *T. gondii,* for example, are kinases with biological activities that include interacting with host signaling pathways (reviewed in (Boothroyd and Dubremetz, 2008; Lim *et al.*, 2012), subverting host cell function (Bradley and Sibley, 2007) and interfering with host cell immunity (Fentress *et al.*, 2010; Ong *et al.*, 2010; Steinfeldt *et al.*, 2010; Niedelman *et al.*, 2012; Yamamoto and Takeda, 2012), processes which are crucial for these parasites to survive within nucleated host cells and establish a chronic infection (Fox *et al.*, 2016). Conversely, none of the known *Plasmodium* ROPs have been shown to have kinase activity. The extrapolation of functional insights gained from *Toxoplasma* ROPs to *Plasmodium* is hindered by the lack of conservation between the *Toxoplasma* and *Plasmodium* ROPs and by the very different host cells in which these parasites reside. To date, *Plasmodium* ROPs have been assigned roles that include rhoptry biogenesis (Topolska

et al., 2004; Kats *et al.*, 2006), host cell invasion (Werner *et al.*, 1998; Topolska *et al.*, 2004), PV formation (Hiller *et al.*, 2003a) and host cell modification (Trenholme *et al.*, 2000; Nguitragool *et al.*, 2011), however, functional data supporting these roles are limited in the literature.

One of the *Plasmodium* protein complexes that initially localizes to the rhoptry bulb is the rhoptry-associated protein (RAP) complex. Members of this complex are highly abundant and consist of non-covalently associated proteins that include RAP1 and either RAP2 or RAP3 in *P. falciparum* (Howard and Reese, 1990). RAP2 and RAP3 are paralogs, deriving from a gene duplication event in an ancestor of *P. falciparum* (Baldi *et al.*, 2002). Other human malaria species and the rodent malaria species harbour only a single RAP2/3 gene.

The *P. falciparum* (*Pf*) RAP complex has been previously implicated in host cell invasion as antibodies and peptides directed against *Pf*RAP1 and *Pf*RAP2 inhibited erythrocyte invasion *in vitro* (Schofield *et al.*, 1986; Harnyuttanakorn *et al.*, 1992; Howard *et al.*, 1998). Moreover, individuals naturally exposed to *P. falciparum* develop antibodies against RAP1 (Jakobsen *et al.*, 1997; Stowers *et al.*, 1997; Fonjungo *et al.*, 1999) and monkeys immunised with RAP1 and RAP2 are partially protected against a challenge infection (Perrin *et al.*, 1985; Ridley *et al.*, 1990). However, this protection is inconsistent with our present knowledge regarding the sequence of events during *P. falciparum* invasion, in which the ROPs are secreted after the tight junction has formed and thus are inaccessible to antibodies (Riglar *et al.*, 2011). Moreover, truncation of RAP1 in *P. falciparum* did not affect the ability of parasites to invade erythrocytes, nor their growth within erythrocytes (Baldi *et al.*, 2000; Baldi *et al.*, 2002)(Baldi *et al.*, 2000; Baldi *et al.*, 2002)(Baldi *et al.*, 2000; Baldi *et*

al., 2002) although RAP2 trafficking was impaired, indicating RAP2 is non-essential for *P. falciparum* survival *in vitro* (Baldi *et al.*, 2000). However, it is possible that RAP3 was able to complement RAP2 function in this line, although this was not formally proven. Subsequent attempts to disrupt *RAP1* in other *P. falciparum* lines like 3D7, W2mef and HB3 strains have been unsuccessful (D. Baldi, personal communication), suggesting that RAP1 may provide an important advantage for these parasites.

Interestingly, attempts to knock out *RAP2/3* in the rodent malaria strain *P. berghei* using standard targeted gene disruption technology have not been successful (Janse *et al.*, 2011). This suggests that RAP2/3 may play an essential role for asexual blood stage development *in vivo*. In light of this, we attempted to dissect the functional roles of the RAP complex *in vivo* using a combination of gene knockout, gene tagging and conditional knockdown approaches in *P. berghei*. In conjunction, we have undertaken detailed characterization of RAP1 in *P. falciparum.* This study provides proof that RAPs are not involved in the invasion of host erythrocytes *in vivo*. Instead we present evidence supporting a post-invasion role for the RAP complex in helping to remodel the interface between the parasite and host cell to ensure intra-erythrocytic growth and survival of *Plasmodium* parasites *in vivo*.

RESULTS

RAP1 is critical for P. berghei survival in vivo

As there are no previous reports as to whether RAP1 is essential for parasite survival *in vivo*, this gene was targeted for deletion in *P. berghei* to generate a loss-of-function mutant. The targeting construct pL0048_RAP1 was designed to replace the endogenous RAP1 gene with the hDHFR-yFCU selectable marker cassette via double cross over homologous recombination at the 5' and 3' targeting sequence (Fig. S1A). Although the first two transfection experiments did not yield any parasites after drug selection with pyrimethamine, pyrimethamine-resistant parasites were recovered after the third transfection attempt. However, Southern blot analysis revealed that the recovered parasites were wild type parasites harbouring the episomal version of the targeting construct and no band indicative of the correct integration event was observed (Fig. S1B).

To assess whether the RAP1 locus is in fact amenable to gene targeting, we next attempted to epitope tag the endogenous gene in *P. berghei* with a triple haemagglutinin (HA) epitope and single streptavidin tag using a 3′ replacement strategy (Fig. S2A). Diagnostic PCR (Fig. S2B) and Southern blot analysis (Fig. S2C) of genomic DNA (gDNA) harvested from parasites resistant to pyrimethamine after transfection of the linearised pRAP1-HA tagging construct revealed bands indicative of a successful 5' and 3' recombination event in a population of the transgenic parasites, which were absent from the wildtype line. Western blot analysis of parasite extracts harvested from the blood of infected mice confirmed RAP1 had been epitope-tagged as the anti-HA reacted with a protein species around the predicted molecular mass of RAP1 (86 k Da) fused to the epitope tag (4.5 kDa) in

the transgenic parasite line, with no labelling observed in control *P. berghei* wild-type lysates as expected (Fig. S2D). While a monoclonal antibody that has been raised against *P. falciparum* RAP1 (anti-*Pf*RAP1) (Schofield *et al.*, 1986) did not react well against *P. berghei* ANKA parasites lysates by Western blot (data not shown) (in which there is 31% amino acid identity and 78 % similarity between the two proteins), immunofluorescence analysis (IFA) using the anti-HA antibody in conjunction with the anti-*Pf*RAP1 antibody on schizont-stages showed that the anti-*Pf*RAP1 and anti-HA labelling co-localized, giving the same punctate labelling pattern typical of rhoptry localisation (Fig. S2E). These experiments corroborated that RAP1 could be epitope tagged in *P. berghei* and thus the failure to genetically disrupt RAP1 suggests that this protein is highly likely to be critical for parasite growth and survival *in vivo*.

Conditional regulation of RAP1 and RAP2 expression in P. berghei

As the RAP1 gene could not be genetically deleted in *P. berghei*, a transgenic *P. berghei* parasite line, termed *Pb*RAP1 iKD was created in which the *RAP1* gene was placed under the transcriptional control of a conditional tetracycline (Tet) transcriptional regulation system (Pino *et al.*, 2012), which allows *RAP1* transcription to be regulated by the addition of anhydrotetracycline (ATc) (Fig. 1A). After transfection of *P. berghei* with the pRAP1 iKD targeting construct, transgenic parasites could be recovered within 12 days of commencing pyrimethamine selection. These parasites were assessed for integration by diagnostic PCR (Fig. 1B) and Southern blot analysis (Fig. 1C), which confirmed successful integration of the construct into the endogenous *RAP1* gene locus.

In addition, since *P. berghei RAP2* had already been shown to be refractory to genetic ablation via conventional knockout strategies (Janse *et al.*, 2011), we directly opted for a conditional knock down strategy to assess its function *in vivo*. Thus similar to RAP1, a PbRAP2 iKD line was constructed using the ATc-regulatable system. Correct integration of the targeting construct to the endogenous RAP2 locus was assessed by diagnostic PCR (Fig. 1B) and confirmed by Southern blot analysis (Fig. 1D).

The level of knockdown of RAP1 and RAP2 at the transcriptional level was next analysed in the *Pb*RAP1 iKD and *Pb*RAP2 iKD lines, respectively by quantitative reverse transcriptase PCR (qRT-PCR). For these experiments, ring-stage parasites that had been harvested from infected mice were cultured in the absence or presence of 1 μg/ml ATc until schizont stage, from which the abundance of *RAP1* or *RAP2* transcript was measured relative to *GAPDH* as a control. These experiments revealed treatment with ATc led to a 3.7-fold down regulation of RAP1 (Fig. 2A) and 2.4-fold down regulation of RAP2 gene expression (Fig. 2B), respectively. IFA experiments using anti-*Pf*RAP1 and anti-*Pf*RAP2 antibodies revealed RAP1 and RAP2 expression had also been reduced at the translational level in the ATc-treated lines. For *Pb*RAP1 iKD parasites, more than 90 % of parasites grown in the presence of ATc exhibited weak RAP1 labelling relative to parasites grown in the absence of ATc (n=100) (Fig. 2C). Similar results were observed with the *Pb*RAP2 iKD parasites, with 84 % of the parasites treated with ATc showing very faint RAP2 expression compared to the untreated control, and only 16 % showing a strong RAP2 signal comparable to that of untreated parasites (Fig. 2D). Irrespective of the labelling intensity in the knockdown lines, RAP1 and RAP2 appeared to be evenly distributed to each merozoite within individual

schizonts, a similar finding to the residual AMA1 expression observed by IFA after conditional regulation of AMA1 in *P. falciparum* using the dimerizable Cre recombinase (Yap *et al.*, 2014).

Knockdown of RAPs does not alter rhoptry morphology or maturation of merozoites

Since the RAP complex is very abundant in schizont stages, we were interested in whether the absence of either of these proteins had any effect on rhoptry formation. Genetic disruption of ROP1, the major *T. gondii* rhoptry antigen, which shows no sequence similarity to *P. falciparum* RAPs, has been shown to alter rhoptry morphology (Soldati *et al.*, 1995). This was analysed in *Pb*RAP2 iKD parasites in comparison to *P. berghei* ANKA wildtype parasites that had been harvested from mice and treated *in vitro* for 12 hours with either ATc or vehicle control. However, no apparent difference in the electron density or morphology of the rhoptries was observed (Fig. 3A), suggesting that RAP2 is not essential for rhoptry formation in *Plasmodium spp*. Moreover, knockdown of either RAP1 or RAP2 expression did not affect parasite maturation and replication, as there was no significant difference observed in merozoite number or schizont formation compared to parasites grown in the absence of ATc (Fig. 3B).

Trafficking of RAP2 but not other rhoptry proteins is affected by knockdown of RAP1

In *P. falciparum* targeting of the RAP complex to the rhoptry occurs via the N-terminus of RAP1 through an unknown mechanism (Baldi *et al.*, 2000). Thus it was interesting to see the fate of members of the RAP complex as well as other rhoptry proteins in

the *Pb*RAP1and *Pb*RAP2 iKD lines. While IFA analysis of mature, untreated *Pb*RAP1 iKD schizonts and merozoites with anti-RAP2 antibodies revealed a punctate RAP2 labelling typical of rhoptry staining, *Pb*RAP1 iKD parasites that had been treated with ATc showed a diffuse RAP2 staining pattern in schizonts and no labelling in the extracellular merozoites, indicating RAP2 trafficking was impaired (Fig. 3C). In contrast, knocking down the expression of RAP2 did not affect the trafficking of RAP1 (Fig. 3D). The trafficking and distribution of several other rhoptry bulb (RAMA, RhopH3) and neck (RON6) proteins was investigated alongside that of a micronemal protein (AMA1) but the localisation of these proteins were unaffected by the absence of either RAP1 or RAP2 (Fig. S3). This indicates that the RAPs do not play a role in the trafficking of other proteins to the rhoptry.

The RAP complex is not essential for erythrocyte invasion

RAP1 has been previously suggested to play a role in erythrocyte invasion (Schofield *et al.*, 1986; Harnyuttanakorn *et al.*, 1992; Howard *et al.*, 1998), although *P. falciparum* expressing truncated RAP1 can still invade erythrocytes *in vitro*. To verify whether the RAP complex is essential for invasion, *in vitro* invasion assays of the *P. berghei* RAP1 knockdown lines grown in the presence or absence of ATc were performed using two-colour flow cytometric analysis. For this, purified schizont preparations of each parasite line were stained with the DNA dye Hoechst and incubated with donor RBCs harvested from an uninfected BALB/c mouse that had been stained with the amine-reactive fluorescent dye DDAO-SE. Hence cells that stained with both Hoechst and DDAO represent new invasion events, which were expressed as a percentage of donor erythrocytes (Fig. 4A). The analysis revealed that

there was no significant difference in the invasion efficiency of parasites with depleted expression levels of RAP1 and RAP2 (Fig. 4B), confirming that the RAPs are not required for host cell invasion by the *Plasmodium* parasites.

Knocking down RAP expression affects parasite growth in vivo and the development of parasites post-invasion

To assess the effect of RAP1 and RAP2 knockdown on the growth and/or replication of the *Pb*RAP1 iKD and *Pb*RAP2 iKD, BALB/c mice (n=6 per group) pre-exposed to ATc or vehicle control for 24hrs were infected with asynchronous 1×10^6 *P. berghei* ANKA wild type parasites, *Pb*RAP1 iKD or *Pb*RAP2 iKD parasites. From day 3 post-infection (p.i) the parasitaemia from each mouse was calculated on a daily basis. Unlike the growth of parental *P. berghei* ANKA parasites, which was unaffected by the presence of ATc, *Pb*RAP1 iKD and *Pb*RAP2 iKD parasites exposed to ATc grew significantly more slowly than the same parasite lines grown in the absence of ATc (Fig. 5A).

As the trophozoite and schizont stages of the *P. berghei* sequester in the microvasculature of mice, we next analysed parasite growth of the RAP knockdown lines *in vitro* so that all the stages of the parasite growth could be carefully examined to gain insight into the basis for their attenuated growth *in vivo*. For this, purified schizont-stage *Pb*RAP1 iKD and *Pb*RAP2 iKD parasites were intravenously injected into untreated mice or mice pre-exposed to ATc to establish a synchronous infection. The parasites invaded erythrocytes and developed normally into ring stages. Parasites were then harvested from one group of mice at this point (Cycle-I parasites) or after next round of invasion (Cycle-II parasites), and cultured

in vitro in the presence/absence of ATc until schizont stage. Parasite growth and morphology was monitored regularly by observing Giemsa stained blood smears.

Cycle-I parasites of both the transgenic lines grown in the presence of ATc appeared to grow normally and similar to the parasites growing in the absence of ATc (data not shown), consistent with knockdown of *RAP* transcript not occurring until schizont stage in the mouse. Moreover, the parasitaemias in the Giemsa-stained blood smears at the beginning of both Cycle I and Cycle II (Fig. 5B) showed no difference in the levels of invasion with either parasite line, consistent with the results from the *in vitro* invasion assays. However during Cycle-II, the maturation of ~30% of both PbRAP1iKD and PbRAP2iKD rings into mature trophozoites was abrogated in the presence of ATc. A close examination of these parasites revealed abnormal looking trophozoites with stunted morphology. PbRAP1iKD and PbRAP2iKD treated with ATc were consistently localised at the periphery of the erythrocyte and stained more intensely with Giemsa (Fig. 5B and Fig. S4, respectively). By the end of Cycle II, the numbers of ATc-treated parasites relative to non-treated parasites was ~25% less. The onset of schizogony in the remaining knockdown parasites was also delayed, such that at 25 hpi, only 15 % of the RAP1 iKD parasites had developed into schizonts compared to 73 % of parasites grown in the absence of ATc (Fig. 5B). Very similar results were observed for the *Pb*RAP2 iKD parasites (Fig. S4). This indicates that the RAPs play an important role downstream of invasion and are required for parasite growth, such that knocking down their expression affects parasite viability and the duration of the asexual cycle.

Electron microscopy of PbRAP2 knockdown parasites reveals a PVM defect

To further understand the defect in growth in parasites with depleted RAP expression, ultrastructural studies were conducted on the trophozoite stages of the *Pb*RAP2 inducible knockdown parasites and *P. berghei* wildtype parasites (grown both in the presence and absence of ATc) using transmission electron microscopy (TEM). PbRAP2 iKD parasites displayed significant PVM differences, with numerous branched and ruffled reticulations of the parasite membranes extending into the erythrocyte cytosol. In some cases these protrusions appeared to be an extension of the PV only, while in other cases, this bleb appeared to contain parasite cytosol, with the projection containing parasite ribosome-like objects, indicating the parasite membrane may also be affected (Fig. 6). These protrusions often contained regions of distorted membranous ruffles, rather than the smooth tubular extensions (termed tubovesicular network or TVN) occasionally seen in wild type parasites, and previously described in *P. berghei* and other *Plasmodium* species (Matz *et al.*, 2015). Although membranous extensions into the host cell are not completely absent from ATc-untreated parasites, the protrusions in the PbRAP2 iKD parasites are larger, more distorted, and more numerous. Of 60 mid-trophozoite stage parasites scored from each condition, 62% of the ATc treated PbRAP2 iKD parasites had a clear PVM protrusion into the erythrocyte, whereas only 17% of the untreated parasites had any membranous extension. This phenotype in the knockdown parasites suggests that the structure of the PVM is impaired in the absence of RAP2. However, by IFA, no difference in the localisation of the PVM protein, EXP2, could be observed in the PbRAP2 iKD parasites when grown in the presence or absence of ATc (Fig. S5).

RAP1 persists after erythrocyte invasion and is peripherally bound to the PVM

Since the effect of knocking down RAP1 or RAP2 was not apparent until parasites reached the trophozoite stage, further molecular characterisation of RAP1 was performed in *P. falciparum,* for which there is a greater availability of antibodies. An earlier study has already shown that RAP1 is carried into the rings after invasion (Richard *et al.*, 2009), thus IFA analysis was conducted to determine how long RAP1 persists in the newly-formed ring-stage parasite and when new RAP1 is synthesized for the next replication cycle. Our IFA analysis shows that RAP1 persists until the late ring stage (~15 hrs post invasion) but can no longer be detected once the parasite starts forming haemozoin pigment (trophozoite stage) (Fig. 7A). In accordance with published transcriptome data, new RAP1 is not synthesized again until early schizont stage (Fig. 7A) (Bozdech *et al.*, 2003) and newly formed protein localises to the rhoptry with other ROP proteins such as RAMA and RhopH3 (Fig. S3A). The prolonged persistence of RAP1 in the ring stages is in keeping with a functional role downstream of invasion. Differential solubilisation of *P. falciparum* schizont and ring-stage infected erythrocytes revealed that RAP1 was not detected in the soluble fraction after hypotonic lysis but instead required sodium carbonate for extraction. This indicates that RAP1 is peripherally associated with membranes both pre- and post-invasion (Fig. 7B).

To determine the compartment in which RAP1 resides, selective membrane permeabilization was performed in conjunction with a protease protection assay. For this, samples were treated with tetanolysin, which permeabilises the erythrocyte membrane but keeps the PVM intact. Samples were then subjected to digestion with proteinase K. Samples

were then analysed by Western blot (Fig. 7C). This revealed that RAP1 is protected from proteinase K digeston, while the Maurer's cleft protein, Skeleton Binding Protein 1 (SBP1) is cleaved under these conditions, in keeping with previous studies (Cooke *et al.*, 2006). Parasitophorous Vacuole protein 1 (PV1) (Chu *et al.*, 2011) and GAPDH (which resides in the parasite cytoplasm) served as control proteins and their protection from proteinase K digestion demonstrates the integrity of the PVM and parasite membrane. From these results it can be inferred that RAP1 localises to the PV. (Chu *et al.*, 2011)

The RAP interactome

Although RAP1 is required for trafficking of RAP2 (and presumably RAP3) to the rhoptries, it is unknown whether the RAPs still exist as a complex post-invasion and whether they interact with other proteins at the PV or PVM. To investigate, we performed a global analysis of the *P. falciparum* RAP1 interactome at ring-stages by immunoprecipitating RAP1 with anti-*Pf*RAP1 antibodies (with anti-GAPDH antibodies used as a control). The elution fraction containing proteins that affinity purified with RAP1 were separated by SDS-PAGE. Protein bands that were visually unique to the RAP1 pull-down after staining were excised, as were the corresponding gel regions of the negative control and proteins were identified by liquid chromatography-tandem mass spectrometry (LC-MS/MS) (Fig. 8A).

In total we identified 32 parasite proteins that based on total peptide count preferentially interacted with RAP1 (≥4-fold enriched). All members of the RAP complex were detected, as were proteins belonging to the RhopH complex (most notably RhopH2) and RON3 (Fig. 8B). Of proteins that harboured a signal sequence or transmembrane domain, 13

proteins were specifically enriched, as were 6 exported proteins (Tables 1 and 2). Notably, the top hits amongst these proteins were four DNAJ-containing proteins, disulphide isomerases (of which PDI-8 has been previously identified in the PV proteome (Nyalwidhe and Lingelbach, 2006), components of the PTEX export machinery (de Koning-Ward *et al.*, 2009) and other transport proteins. As the ~37 kDa band in the control pull-down that most likely corresponds to GAPDH was not excised from the protein gel, western blotting of the eluates with either anti-*Pf*GAPDH or anti-*Pf*RAP1 was performed. This confirmed that GAPDH and RAP1 had been specifically immunoprecipitated with the corresponding antibody (Fig. 8C). In addition, we confirmed the interaction of RAP1 with the RhopH complex was specific (via *Pf*Rhop3 antibody). In contrast, there was relatively little enrichment of HSP101 when comparing the elution fraction to the unbound fraction or to the elution fraction of the control pull-down, although we note that several other members of the PTEX complex were also affinity purified. With respect to host erythrocyte proteins, we did not expect an enrichment of erythrocyte membrane proteins in the RAP1 pull-down because the bulk of these proteins are excluded from the PVM (Murphy *et al.*, 2004). In fact the only human proteins that were enriched more than four-fold in the RAP pull-down were cytoskeletal proteins 4.1 and 4.2 (Fig. S6).

DISCUSSION

The molecular players involved in the early stages of *Plasmodium* invasion of erythrocytes are beginning to be revealed with the aid of transfection technologies and live cell imaging platforms, in conjunction with the use of antibodies or compounds that block potential invasion ligands/receptors. In comparison, there has been very little progress in our understanding of the functional role of proteins secreted from the rhoptry bulb during invasion, including the RAP complex despite its early identification and being a very abundant complex. Although parasites with a truncated *RAP1* gene have been generated in the D10 strain of *P. falciparum*, functional studies of the RAP complex *in vivo* have been hampered because viable *P. berghei* parasites that lack the *RAP1* (this study) or *RAP2/3* gene (Janse *et al.*, 2011) have not been able to be recovered, even if very long targeting sequences in transfection plasmids generated by recombineering are used to drive homologous integration into the *RAP* locus (Gomes *et al.*, 2015)(http://plasmogem.sanger.ac.uk/). Although we could epitope tag the endogenous *P. berghei RAP1* gene, we note that only a portion of the parasites in the non-clonal population contained the expected integration event, which may be the result of the modification of the RAP1 protein or the *rap*1 locus incurring a fitness cost. This necessitated the use of conditional gene knockdown approaches in this study to conditionally regulate RAP1 and RAP2 expression.

Despite the abundance of the RAP complex during schizogony, knockdown of PbRAP1 or PbRAP2 revealed that neither of these proteins are essential for rhoptry biogenesis, nor are they required for erythrocyte invasion. However, depletion of RAP1 in *P. berghei* affected the trafficking of RAP2 to the rhoptry, consistent with findings in *P.*

falciparum using a RAP1 truncation mutant, which showed RAP1 serves an escorter protein for RAP2 (Baldi *et al.*, 2000). RAP1 is not a general escorter of proteins to the rhoptry, however, as we did not observe defects in the trafficking of other rhoptry proteins after knockdown of PbRAP1, nor after knockdown of PbRAP2.

Following secretion from the rhoptry, RAP1 is injected into the PV and peripherally associates with the PVM where it remains for the duration of ring stages. Immunoprecipitation of *P. falciparum* RAP1 at the ring-stage confirms that the RAP proteins remain together as a complex following their secretion from the rhoptries. Furthermore, the RAP complex associates with members of the higher molecular weight RhopH complex, which like the RAPs are present in detergent-resistant membranes (DRMs) in schizonts (Hiller *et al.*, 2003b; Sanders *et al.*, 2007). After invasion RhopH2 has been shown to insert into the newly forming vacuolar bilayer (Hiller *et al.*, 2003b). RAP1 also affinity purified processed forms of RON3 that are only present in parasites post-invasion (Ito *et al.*, 2011). RON3 is a mis-named protein because unlike other RON proteins which localise to the rhoptry neck and which did not co-precipitate with RAP1, it localises to the rhoptry bulb; moreover, it has been shown to co-localise with RAP1 in the ring-stages by IFA (Ito *et al.*, 2011).

Several other proteins that harbour signal sequences or transmembrane domains were also enriched in the RAP1 pull-down, notably molecular chaperones, components of the PTEX complex (and some known exported proteins), transporters (of which the multidrug resistant protein 2 has been previously localised by IFA to the periphery of the parasite) (Kavishe *et al.*, 2009) and PF3D7_0204100. The latter is a conserved protein of unknown

function containing two trimeric LpxA-like enzyme domains and SelI repeats that typically engage in protein-protein interactions and are commonly found in macromolecular complexes such as those involved in signal transduction pathways. Given that lipid raft-like membranes serve as assembly regions for membrane protein trafficking and signalling molecules, and the RAP complex affinity purified diverse proteins implicated in these functions, the RAP complex may serve as a scaffold to compartmentalise various cellular processes at the interface between the parasite and host cell rather than serving as a molecular component of different complexes *per se*. The PVM ultrastructural defects observed by TEM after depletion of RAP2 from intracellular parasites suggests that the RAP complex at the host-parasite interface contributes to the architecture of the PVM. Since the PVM is formed from the host erythrocyte membrane during invasion (Lingelbach and Joiner, 1998) and parasite proteins are subsequently incorporated into this membrane, it would be expected that interference with this process would lead to altered phenotypes when the parasite is rapidly expanding to accommodate its requirements. Indeed delays in the growth of parasites depleted of RAPs as well as aberrant parasite morphology became apparent by the trophozoite stage of development, which not only led to delayed schizogony but also led to parasite attrition *in vitro* and slower parasite growths *in vivo.*

EXPERIMENTAL PROCEDURES

Ethics

All experiments involving rodents were performed in accordance with the Australian Government and National Health recommendations and the National Health and Medical Research Council Australian code of practice for the care and use of animals for scientific purposes. The protocols were approved by the Animal Welfare Committee at Deakin University (Approval No.: AWC A97/2010, A98/2010 and G37/2013).

Mice infections and growth analysis

Female BALB/c mice aged between 5-8 weeks were randomized into groups and infected intraperitoneally with 10^6 *P. berghei* ANKA infected erythrocytes. The development of parasites within erythrocytes was monitored by visualising Giemsa-stained blood smears. Parasitemias were determined by counting a minimum of 1000 erythrocytes.

For the *in vivo* treatment of parasites with anhydrotetracycline (ATc), mice were randomized into groups of five per experiment (n=2) and 24 hr prior to infection administered with drinking water containing 0.2 mg/ml ATc (Sigma) made in 5 (w/v) % sucrose, with drinking water containing 5% sucrose alone serving as a negative control. Mice were then infected with 10^6 infected erythrocytes and maintained on drinking water containing either ATc or vehicle control for the duration of the experiment. Parasitaemia was calculated on a daily basis from day 3 post-infection (p.i). Mice were humanely culled when parasitaemias exceeded 25%.

For *in vitro* treatment of parasites with ATc, erythrocytes harvested from infected mice were applied to a MACS CS column (Miltenyi Biotec) to remove late stage parasites. The purified ring-stage parasites were cultured to schizont stage in RPMI 1640 medium containing L-glutamine (Life Technologies) supplemented with 25mM HEPES, 0.2% bicarbonate, 20% fetal bovine serum and 1 μg/ml ATc (or vehicle as a control) at 36.5°C for 16 h.

DNA constructs

The sequence of *P. berghei* (*Pb*) *RAP1* (PbANKA_1032100) and *RAP2 /3* (PbANKA_1101400) were retrieved from the on-line *Plasmodium* genome database, PlasmoDB (Aurrecoechea *et al.*, 2009). For targeted gene deletion of *PbRAP1*, fragments of the 5′ UTR and 3′ UTR that would serve as targeting regions to drive integration into the endogenous locus were PCR-amplified from *P. berghei* ANKA genomic DNA (gDNA) using gene-specific primers (163F/164R and 93F/90R). The 5′ UTR and 3′ UTR homologous sequences were digested with *Kpn*I/ *Sal*I and *Sca*I/*Bam*HI, respectively and sequentially inserted into the corresponding sites of the vector pL0048 (Lin *et al.*, 2011) to generate the construct pL0048_RAP1. The construct was sequenced to ensure no mutations had been introduced during the PCR. Prior to transfection, pL0048_RAP1 was digested with the restriction enzymes *Hin*dIII and *Xho*I to remove the vector backbone.

To epitope tag the endogenous *PbRAP1* gene, ~2 Kb of RAP1 coding sequence immediately upstream of the stop codon served as the targeting region for homologous recombination into the *PbRAP1* endogenous locus. This was PCR-amplified from PbANKA gDNA in roughly two equal parts (RAP1a and RAP1b) using the oligonucleotides 186F/187R (5′ targeting

region) and 188F/189R (3′ targeting region). The RAP1 a and b fragments were digested with *Sac*II/*Spe*I and *Spe*I/*Avr*II, respectively and sequentially inserted into the corresponding sites of the vector pB3 vector (Waters *et al.*, 1997). This created a *Spe*I site between the two adjacent 5′ and 3′ sequences that would later be used to linearize the DNA prior to transfection into *P. berghei* ANKA, and placed a triple hemagglutinin (HA) epitope tag adjacent to the 3′ targeting region of RAP1, to give the final epitope-tagging construct, pRAP1-HA.

The targeting vector for inducible knockdown of *PbRAP1* and *PbRAP2* was based on pPRF-TRAD4-Tet07-HAPRFhDHFR (Pino *et al.*, 2012) that had been modified to include a *Nhe*I restriction site downstream of the profiling coding sequence and a *Bss*HII restriction enzyme site between the profilin 5′ untranslated region and the TRAD4 sequence (Elsworth *et al.*, 2014). This enabled cloning of the first 1.5 kilobases (kb) of the RAP1 coding sequence including its signal sequence (amplified with 91F/75R) into the *Pst*I and *Nhe*I sites and 1.3 kb of the RAP1 5′ untranslated region (amplified using oligonucleotides 76F/77R) into the *Nhe*I and *Bss*HII sites. For the RAP2 inducible knockout construct, the first 1.67 kb of the RAP2 cds (amplified with 147F/83R) and 1.15 kb of the RAP2 5′ untranslated region (amplified with 80F/156R) was cloned into the *Pst*I/*Nhe*I and *Nhe*I/*Bss*HII sites of the modified pPRF-TRAD4-Tet07-HAPRFhDHFR vector, respectively. Prior to transfection, the constructs were linearized with *Nhe*I.

Parasite transfection

Transfection of *P. berghei* and selection of the transgenic parasites was performed as previously described (Janse *et al.*, 2006). Briefly, Nycodenz (Axis-Shield) -purified *P.*

berghei schizonts were prepared for transfection and DNA constructs were introduced using the Nucleofector® electroporation device (AMAXA). The resulting DNA mixture was injected intravenously into 6- to 8-week-old BALB/c mice and drug selection with pyrimethamine (0.07 mg ml−1) of genetically transformed parasites begun at day 1 post transfection.

Nucleic acid analysis

Correct 5′ and 3′ integration of the transfected plasmids into the respective *P. berghei* endogenous gene locus was analysed by diagnostic PCR on parasite DNA isolated from infected rodent blood. The following oligonucleotide combinations were used for this analysis: Pb RAP13XHA: a-154F/b-233R, c-45F/d-311R; PbiRAP1KD: a-181F/b-T51R, c-213F/d-311R; PbiRAP2KD: a-183F/b-T51R, c-213F/d-182R. The genotypes of the transgenic parasite line were confirmed by Southern blot analysis. Nucleic acid probes were synthesized using the DIG PCR Probe Synthesis kit (Roche) and detection was performed with the DIG Luminescent Detection kit (Roche) in accordance with the manufacturer's protocol.

To detect the level of the gene knockdown at the transcriptional level, quantitative real time (qRT) PCR was performed. RNA was extracted from the blood stage parasites using Trisure (Invitrogen) followed by treatment with DNaseI (Invitrogen). cDNA was then made using the Omniscript RTKit (Qiagen) in accordance with the manufacturer's protocol. The cDNA of the ATc-treated and untreated parasites was used in PCR reactions using the oligonucleotides to detect RAP1 (527F/528R and 529F/530R), RAP2 (569/570 and 571/572) and parasite GAPDH (567F/568R) as the reference gene. The expression levels of *RAP1* and *RAP2* were

normalised against the *gapdh* house-keeping gene, with gene expression values calculated based on the 2ΔΔCt method.

Western blot analysis

For immunoblots, infected rodent blood was collected and depleted of leucocytes by passage through a CF11 column (Whatman) and then lysed using 0.02% saponin for 15 min on ice, followed by centrifugation at 20 000 *g* for 5 min. After three washes with ice-cold mouse tonicity (MT) PBS (150 mM NaCl, 16 mM Na_2HPO_4, 4 mM NaH_2PO_4) containing 1× complete protease inhibitors (Roche), the parasite pellet was resuspended in 1× reducing sample buffer. Parasite lysates were separated on 4–12% gradient SDS-PAGE gels (Invitrogen) and transferred onto 0.45 µm nitrocellulose membrane (Millipore) using SDS transfer buffer with methanol and a wet transfer blotting device (Bio-Rad). The membranes were blocked in 5 (w/v) % skim milk in PBS and probed with mouse *P. falciparum* anti-RAP1 (1:3000 dilution), rabbit anti-*Pf*RAMA-D (1:3000 dilution), rabbit anti-*Pf*EXP2 (1:1000 dilution), rabbit anti-*Pf*HSP101(1:1000 dilution), rabbit anti-*Pf*SERA5 (1:1000 dilution), anti-*Pf*RhopH3 (1:1000) or rabbit anti-HA (1:1000). Detection was performed using Super Signal enhanced chemiluminescence (Thermo Fischer Scientific).

Differential solubility analysis

P. falciparum-infected erythrocytes (rings or schizonts) at 5 % parasitaemia were saponin lysed (0.02%) and the resulting pellet after centrifugation at 5000 *g* was resuspended in 600 µL hypotonic lysis buffer (1mM HEPES, pH 7.4), containing complete protease inhibitor cocktail (Roche) and incubated at 4°C for 30 mins. The lysate was centrifuged at 100 000 *g*

for 30 mins at 4°C and the supernatant representing soluble protein fraction was collected. The pellet was resuspended in 500 µl 0.1M Na2CO3 (pH 11.5), and kept on ice for 30 min to extract peripheral membrane proteins, which are present in the supernatant fraction after centrifugation at 100 000 *g* for 30 mins at 4°C. To extract integral membrane proteins, the resulting pellet was treated with 1% Triton X-100 on ice for 30 min and then centrifuged again at 100 000 *g* for 30 mins at 4°C. Equivalent amounts of the samples were analysed by Western blot.

Protease protection assay

Aliquots of *P. falciparum*-ring stage parasites (~$5x10^7$) were treated with 3 U of tetanolysin (purchased from Sigma and resuspended in PBS) for 10 min at room temperature with vigorous shaking at 600 rpm. Half of the aliquots were then treated with 20 µg/ml proteinase K for 20 min at 37°C with shaking at 600 rpm. Protease inhibitor cocktail (Roche, 10x) + 1 mM PMSF was then added to each aliquot and the samples incubated for a further 3 min. After centrifugation at 2000 *g*, the pellets were resuspended in reducing sample buffer and analysed by Western blot. Antibodies raised against *P. falciparum* SBP1, and GAPDH were all used at 1:1000.

Immunofluorescence analysis

For immunofluorescence analysis (IFA), erythrocytes infected with *P. berghei* were fixed with ice-cold 90% acetone/10% methanol for 2 min. All antibody incubations were performed in 3% BSA/PBS. Primary antibodies for *P. berghei* blood stages were used at the following concentrations: rabbit anti-HA (1:500)(Sigma), mouse anti-*Pf*RAP1 (7H8/50)

(Schofield *et al.*, 1986) (1:300), mouse anti- *Pf*RAP2 (7B2/1H1)(1:200), rabbit anti-*Pf*RAMA-D (Topolska *et al.*, 2004) (1:300), rabbit anti- *Pf*RhopH3 (1:300)(gift from Ross Coppel), rabbit anti- *Pf*RON6 (1:300), mouse anti- *Pf*AMA1 (1:300), rabbit anti-*Pb*MSP1 (1:1000)(de Koning-Ward *et al.*, 2003), rabbit anti- *Pf*RESA (1:2000)(gift from Robin Anders) and rabbit anti- *Pf*EXP2 (1:500). After three washes with mouse tonicity PBS, the appropriate Alexa Fluor 488/568-conjugated secondary antibodies were used at 1:2000 (Molecular Probes) with DAPI (0.5 □g/ml). Images were acquired with an Olympus IX70, Leica TCS SP2 microscope and images were processed using NIH ImageJ version 1.47d (http://rsbweb.nih.gov/ij/) or Adobe CS6 Photoshop.

Quantitation of parasite invasion of erythrocytes using flow cytometry

Schizont stage parasites were stained for 20 mins at room temperature in the dark with the DNA dye Hoechst 34580 (2 μM) (Invitrogen) made in RPMI-1640. After staining, the cells were washed three times with 1 × PBS. In parallel, erythrocytes (BALB/c mouse blood for *P. berghei* assays) were labelled with 10 μM amine-reactive fluorescent dye 7-hydroxy-9H-(1,3-dichloro-9,9-dimethylacridin-2-one) succinimidyl ester (Cell Trace Far Red DDAO-SE) (Invitrogen) in RPMI-1640 for 1 h at 37°C according to manufacturer's protocol. The stained schizonts and erythrocytes were mixed in the ratio of 1:50, then shaken at 250 rpm for 60 mins in the dark prior to washing 3 times in PBS. Stained samples were examined using a BD FACS Canto II flow cytometer (BD Biosciences). Hoechst 34580 was excited using the 405 nm laser and detected through a 460/50 filter, whilst DDAO was excited by using the 633 laser and detected through 660/20 filter. For each sample, 100,000 events were recorded. The collected data was then further analysed with FlowJo software (Tree Star, Ashland, Oregon).

The number of double positive cells (representing erythrocytes invaded by parasites and typically in the range of 0.3-1%) compared to uninfected DDAO-SE singly-stained erythrocytes was calculated. Experiments were carried out in triplicate and the data presented as the mean ± SEM. GraphPad Prism (GraphPad Software, La Jolla, CA) was used to plot the data and to statistically analyse the data.

Immunoprecipitation

Synchronised ring-stage *P. falciparum* parasites were applied to a MACS CS column (Miltenyi Biotec) to remove any contaminating late stage parasites and then lysed with 0.02% (w/v) in PBS. Pelleted parasite material was resuspended in 1% (v/v) Triton X-100 in PBS containing cOmplete™ protease inhibitors (Roche). After a 30 minute incubation on ice, the material was centrifuged at 17,000 *g* for 10 minutes at 4°C. Protein G–conjugated agarose beads (30 µL) that had been precleared with parasite lysate was then added to parasite lysate that had been incubated overnight at 4°C with either monoclonal anti-*Pf*RAP1 or rabbit anti-*Pf*GAPDH. After a further 4 hour incubation at 4˚C, the mixture was placed on a spin column (Biorad) and unbound material was collected by gravity flow. Beads were then washed twice with 1 mL 0.5% (w/v) Triton X-100 in PBS containing cOmplete™ protease inhibitors (Roche). Bound proteins were eluted with 100 µL 1x non-reducing sample buffer and the proteins were electrophoresed by SDS-PAGE. After staining the gel with Imperial Protein Stain (Thermo Scientific), bands that appeared to be unique to the RAP1 pull-down were excised as was the corresponding area of the gel from the GAPDH pull down to identify affinity purified proteins by mass spectrometry.

Mass spectrometry

Protein bands manually excised from preparative SDS-PAGE gels were subjected to manual in-gel reduction, alkylation, and tryptic digestion as previously described (Matthews *et al.*, 2013). Extracted peptides were injected and fractionated by nanoflow reversed-phase liquid chromatography on an Orbitrap Lumos mass spectrometer (Thermo Scientific) fitted with nanoflow reversed-phase-HPLC (Ultimate 3000 RSLC, Dionex). The nano-LC system was equipped with an Acclaim Pepmap nano-trap column and an Acclaim Pepmap RSLC analytical column. 1 μL of the peptide mix was loaded onto the enrichment (trap) column at an isocratic flow of 5 μL/min of 3% CH_3CN containing 0.1% formic acid for 6 min before the enrichment column was switched in-line with the analytical column. The eluents used for the LC were 0.1% v/v formic acid (solvent A) and 100% CH_3CN/0.1% formic acid v/v (solvent B). The gradient used was 3% B to 20% B for 95 min, 20% B to 40% B in 10 min, 40% B to 80% B in 5 min and maintained at 80% B for the final 5 min before equilibration for 10 min at 3% B prior to the next sample. The mass spectrometer was equipped with a NanoEsi nano-electrospray ion source (Thermo Fisher, USA) for automated MS/MS. The resolution was set to 120000 at MS1 with lock mass of 445.12003 with HCD Fragmentation and MS2 scan in ion trap. The top 3 second method was used to select species for fragmentation. Singly charged species were ignored and an ion threshold triggering at 1e4 was employed. CE voltage was set to 1.9kv

Transmission electron microscopy

P. berghei trophozoite or schizont stage parasites were fixed in 1% glutaraldehyde in RPMI-HEPES on ice for 60 min. Samples were washed in RPMI HEPES and water, then transferred to low-melt agarose before being dehydrated in ethanol, and embedded in LR White Resin (ProSciTech). Resin was heat polymerized, then 90-100nm sections were cut, post-stained with uranyl acetate (6 min) and lead citrate (12 min), and viewed on a Tecnai Spirit transmission electron microscope at 120kV.

Statistics

All graphs and data generated in this study were analysed using GraphPad Prism6.0b Software (MacKiev). A Student's *t*-test using parametric distribution was used to measure differences in parasite growth and replication, RAP1 and RAP2 knockdown and erythrocyte invasion. A P value < 0.05 was considered significant.

REFERENCES

Alexander, D.L., Mital, J., Ward, G.E., Bradley, P. and Boothroyd, J.C. (2005). Identification of the moving junction complex of *Toxoplasma gondii*: a collaboration between distinct secretory organelles. *PLoS Pathog* **1:** e17.

Aurrecoechea, C., Brestelli, J., Brunk, B.P., Dommer, J., Fischer, S., Gajria, B., *et al.* (2009). PlasmoDB: a functional genomic database for malaria parasites. *Nucleic Acids Res* **37:** D539-543.

Baldi, D.L., Andrews, K.T., Waller, R.F., Roos, D.S., Howard, R.F., Crabb, B.S., *et al.* (2000). RAP1 controls rhoptry targeting of RAP2 in the malaria parasite *Plasmodium falciparum*. *EMBO J* **19:** 2435-2443.

Baldi, D.L., Good, R., Duraisingh, M.T., Crabb, B.S. and Cowman, A.F. (2002). Identification and disruption of the gene encoding the third member of the low-molecular-mass rhoptry complex in *Plasmodium falciparum*. *Infect Immun* **70:** 5236-5245.

Bannister, L.H., Hopkins, J.M., Fowler, R.E., Krishna, S. and Mitchell, G.H. (2000). Ultrastructure of rhoptry development in *Plasmodium falciparum* erythrocytic schizonts. *Parasitology* **121 (Pt 3):** 273-287.

Boothroyd, J.C. and Dubremetz, J.F. (2008). Kiss and spit: the dual roles of *Toxoplasma* rhoptries. *Nat Rev Microbiol* **6:** 79-88.

Bozdech, Z., Llinas, M., Pulliam, B.L., Wong, E.D., Zhu, J. and DeRisi, J.L. (2003). The transcriptome of the intraerythrocytic developmental cycle of *Plasmodium falciparum*. *PLoS Biol* **1:** E5.

Bradley, P.J. and Sibley, L.D. (2007). Rhoptries: an arsenal of secreted virulence factors. *Curr Opin Microbiol* **10:** 582-587.

Bradley, P.J., Ward, C., Cheng, S.J., Alexander, D.L., Coller, S., Coombs, G.H., *et al.* (2005). Proteomic analysis of rhoptry organelles reveals many novel constituents for host-parasite interactions in *Toxoplasma gondii*. *J Biol Chem* **280:** 34245-34258.

Cao, J., Kaneko, O., Thongkukiatkul, A., Tachibana, M., Otsuki, H., Gao, Q., *et al.* (2009). Rhoptry neck protein RON2 forms a complex with microneme protein AMA1 in Plasmodium falciparum merozoites. *Parasitol Int* **58:** 29-35.

Chu, T., Lingelbach, K. and Przyborski, J.M. (2011). Genetic evidence strongly support an essential role for PfPV1 in intra-erythrocytic growth of *P. falciparum*. *PLoS One* **6:** e18396.

Cooke, B.M., Buckingham, D.W., Glenister, F.K., Fernandez, K.M., Bannister, L.H., Marti, M., *et al.* (2006). A Maurer's cleft-associated protein is essential for expression of the major malaria virulence antigen on the surface of infected red blood cells. *J Cell Biol* **172:** 899-908.

Counihan, N., Kalanon, M., Coppel, R. and de Koning-Ward, T.F. (2013). *Plasmodium* rhoptry proteins: why order is important. *Trends Parasitol* **29:** 228-236.

de Koning-Ward, T.F., Dixon, M.W.A., Tilley, L. and Gilson, P.R. (2016). *Plasmodium* species: master renovators of their host cells. *Nature Rev Microbiol* **14:** 494-507.

de Koning-Ward, T.F., Gilson, P.R., Boddey, J.A., Rug, M., Smith, B.J., Papenfuss, A.T., *et al.* (2009). A newly discovered protein export machine in malaria parasites. *Nature* **459:** 945-949.

de Koning-Ward, T.F., O'Donnell, R.A., Drew, D.R., Thomson, R., Speed, T.P. and Crabb, B.S. (2003). A new rodent model to assess blood stage immunity to the *Plasmodium falciparum* antigen merozoite surface protein 1_{19} reveals a protective role for invasion inhibitory antibodies. *J. Exp. Med.* **198:** 869-875.

Duraisingh, M.T., Triglia, T., Ralph, S.A., Rayner, J.C., Barnwell, J.W., McFadden, G.I., *et al.* (2003). Phenotypic variation of *Plasmodium falciparum* merozoite proteins directs receptor targeting for invasion of human erythrocytes. *EMBO J.* **22:** 1047-1057.

Elsworth, B., Matthews, K., Nie, C.Q., Kalanon, M., Charnaud, S.C., Sanders, P.R., *et al.* (2014). PTEX is an essential nexus for protein export in malaria parasites. *Nature* **511:** 587-591.

Fentress, S.J., Behnke, M.S., Dunay, I.R., Mashayekhi, M., Rommereim, L.M., Fox, B.A., *et al.* (2010). Phosphorylation of immunity-related GTPases by a *Toxoplasma gondii*-secreted kinase promotes macrophage survival and virulence. *Cell Host Microbe* **8:** 484-495.

Fonjungo, P.N., Elhassan, I.M., Cavanagh, D.R., Theander, T.G., Hviid, L., Roper, C., *et al.* (1999). A longitudinal study of human antibody responses to *Plasmodium falciparum* rhoptry-associated protein 1 in a region of seasonal and unstable malaria transmission. *Infect Immun* **67:** 2975-2985.

Fox, B.A., Rommereim, L.M., Guevara, R.B., Falla, A., Hortua Triana, M.A., Sun, Y., *et al.* (2016). The *Toxoplasma gondii* rhoptry kinome is essential for chronic infection. *mBio* **7**.

Gomes, A.R., Bushell, E., Schwach, F., Girling, G., Anar, B., Quail, M.A., *et al.* (2015). A Genome-scale vector resource enables high-throughput reverse genetic screening in a malaria parasite. *Cell Host Microbe* **11:**404-413

Harnyuttanakorn, P., McBride, J.S., Donachie, S., Heidrich, H.G. and Ridley, R.G. (1992). Inhibitory monoclonal antibodies recognise epitopes adjacent to a proteolytic cleavage site on the RAP-1 protein of *Plasmodium falciparum*. *Mol Biochem Parasitol* **55:** 177-186.

Hayton, K., Gaur, D., Liu, A., Takahashi, J., Henschen, B., Singh, S., *et al.* (2008). Erythrocyte binding protein PfRH5 polymorphisms determine species-specific pathways of *Plasmodium falciparum* invasion. *Cell Host Microbe* **4:** 40-51.

Hiller, N., Akompong, T., Morrow, J., Holder, A. and Haldar, K. (2003a). Identification of a stomatin orthologue in vacuoles induced in human erythrocytes by malaria parasites. A role for microbial raft proteins in apicomplexan vacuole biogenesis. *J Biol Chem* **278:** 48413-48421.

Hiller, N.L., Akompong, T., Morrow, J.S., Holder, A.A. and Haldar, K. (2003b). Identification of a stomatin orthologue in vacuoles induced in human erythrocytes by malaria parasites. A role for microbial raft proteins in apicomplexan vacuole biogenesis. *J Biol Chem* **278:** 48413-48421.

Howard, R.F., Jacobson, K.C., Rickel, E. and Thurman, J. (1998). Analysis of inhibitory epitopes in the *Plasmodium falciparum* rhoptry protein RAP-1 including identification of a second inhibitory epitope. *Infect-Immun* **66:** 380-386.

Howard, R.F. and Reese, R.T. (1990). *Plasmodium falciparum*: hetero-oligomeric complexes of rhoptry polypeptides. *Exp Parasitol* **71:** 330-342.

Ito, D., Han, E.T., Takeo, S., Thongkukiatkul, A., Otsuki, H., Torii, M., *et al.* (2011). Plasmodial ortholog of *Toxoplasma gondii* rhoptry neck protein 3 is localized to the rhoptry body. *Parasitol Int* **60:** 132-138.

Jakobsen, P.H., Kurtzhals, J.A., Riley, E.M., Hviid, L., Theander, T.G., Morris-Jones, S., *et al.* (1997). Antibody responses to Rhoptry-Associated Protein-1 (RAP-1) of *Plasmodium falciparum* parasites in humans from areas of different malaria endemicity. *Parasite Immunol* **19:** 387-393.

Janse, C.J., Kroeze, H., van Wigcheren, A., Mededovic, S., Fonager, J., Franke-Fayard, B., *et al.* (2011). A genotype and phenotype database of genetically modified malaria-parasites. *Trends Parasitol* **27:** 31-39.

Janse, C.J., Ramesar, J. and Waters, A.P. (2006). High-efficiency transfection and drug selection of genetically transformed blood stages of the rodent malaria parasite *Plasmodium berghei*. *Nat Protoc* **1:** 346-356.

Kaneko, O., Mu, J., Tsuboi, T., Su, X. and Torii, M. (2002). Gene structure and expression of a Plasmodium falciparum 220-kDa protein homologous to the *Plasmodium vivax* reticulocyte binding proteins. *Mol Biochem Parasitol* **121:** 275-278.

Kats, L.M., Black, C.G., Proellocks, N.I. and Coppel, R.L. (2006). *Plasmodium* rhoptries: how things went pear-shaped. *Trends Parasitol* **22:** 269-276.

Kavishe, R.A., van den Heuvel, J.M., van de Vegte-Bolmer, M., Luty, A.J., Russel, F.G. and Koenderink, J.B. (2009). Localization of the ATP-binding cassette (ABC) transport proteins PfMRP1, PfMRP2, and PfMDR5 at the *Plasmodium falciparum* plasma membrane. *Malar J* **8:** 205.

Lamarque, M., Besteiro, S., Papoin, J., Roques, M., Vulliez-Le Normand, B., Morlon-Guyot, J., *et al.* (2011). The RON2-AMA1 interaction is a critical step in moving junction-dependent invasion by apicomplexan parasites. *PLoS Pathog* **7:** e1001276.

Lim, D.C., Cooke, B.M., Doerig, C. and Saeij, J.P. (2012). *Toxoplasma* and *Plasmodium* protein kinases: roles in invasion and host cell remodelling. *Int J Parasitol* **42:** 21-32.

Lin, J.W., Annoura, T., Sajid, M., Chevalley-Maurel, S., Ramesar, J., Klop, O., *et al.* (2011). A novel 'Gene Insertion/Marker Out' (GIMO) method for transgene expression and gene complementation in rodent malaria parasites. *PLoS One* **6:** e29289.

Lingelbach, K. and Joiner, K.A. (1998). The parasitophorous vacuole membrane surrounding *Plasmodium* and *Toxoplasma*: an unusual compartment in infected cells. *J Cell Sci* **111 (Pt 11):** 1467-1475.

Matthews, K., Kalanon, M., Chisholm, S.A., Sturm, A., Goodman, C.D., Dixon, M.W., *et al.* (2013). The *Plasmodium* translocon of exported proteins (PTEX) component thioredoxin-2 is important for maintaining normal blood-stage growth. *Mol Microbiol* **89:** 1167-1186.

Matz, J.M., Goosmann, C., Brinkmann, V., Grutzke, J., Ingmundson, A., Matuschewski, K., *et al.* (2015). The *Plasmodium berghei* translocon of exported proteins reveals spatiotemporal dynamics of tubular extensions. *Scientific reports* **5:** 12532.

Murphy, S.C., Samuel, B.U., Harrison, T., Speicher, K.D., Speicher, D.W., Reid, M.E., *et al.* (2004). Erythrocyte detergent-resistant membrane proteins: their characterization and selective uptake during malarial infection. *Blood* **103:** 1920-1928.

Nguitragool, W., Bokhari, A.A., Pillai, A.D., Rayavara, K., Sharma, P., Turpin, B., *et al.* (2011). Malaria parasite clag3 genes determine channel-mediated nutrient uptake by infected red blood cells. *Cell* **145:** 665-677.

Niedelman, W., Gold, D.A., Rosowski, E.E., Sprokholt, J.K., Lim, D., Farid Arenas, A., *et al.* (2012). The rhoptry proteins ROP18 and ROP5 mediate *Toxoplasma gondii* evasion of the murine, but not the human, interferon-gamma response. *PLoS Pathog* **8:** e1002784.

Nyalwidhe, J. and Lingelbach, K. (2006). Proteases and chaperones are the most abundant proteins in the parasitophorous vacuole of *Plasmodium falciparum*-infected erythrocytes. *Proteomics* **6:** 1563-1573.

Oakes, R.D., Kurian, D., Bromley, E., Ward, C., Lal, K., Blake, D.P., *et al.* (2013). The rhoptry proteome of *Eimeria tenella* sporozoites. *Int J Parasitol* **43:** 181-188.

Ong, Y.C., Reese, M.L. and Boothroyd, J.C. (2010). *Toxoplasma* rhoptry protein 16 (ROP16) subverts host function by direct tyrosine phosphorylation of STAT6. *J Biol Chem* **285:** 28731-28740.

Perrin, L.H., Merkli, B., Gabra, M.S., Stocker, J.W., Chizzolini, C. and Richle, R. (1985). Immunization with a *Plasmodium falciparum* merozoite surface antigen induces a partial immunity in monkeys. *J Clin Invest* **75:** 1718-1721.

Pino, P., Sebastian, S., Kim, E.A., Bush, E., Brochet, M., Volkmann, K., *et al.* (2012). A tetracycline-repressible transactivator system to study essential genes in malaria parasites. *Cell Host Microbe* **12:** 824-834.

Proellocks, N.I., Coppel, R.L. and Waller, K.L. (2010). Dissecting the apicomplexan rhoptry neck proteins. *Trends Parasitol* **26:** 297-304.

Rayner, J.C., Galinski, M.R., Ingravallo, P. and Barnwell, J.W. (2000). Two *Plasmodium falciparum* genes express merozoite proteins that are related to *Plasmodium vivax* and *Plasmodium yoelii* adhesive proteins involved in host cell selection and invasion. *Proc Natl Acad Sci U S A* **97:** 9648-9653.

Rayner, J.C., Vargas-Serrato, E., Huber, C.S., Galinski, M.R. and Barnwell, J.W. (2001). A *Plasmodium falciparum* homologue of *Plasmodium vivax* reticulocyte binding protein (PvRBP1) defines a trypsin-resistant erythrocyte invasion pathway. *J Exp Med* **194:** 1571-1581.

Richard, D., Kats, L.M., Langer, C., Black, C.G., Mitri, K., Boddey, J.A., *et al.* (2009). Identification of rhoptry trafficking determinants and evidence for a novel sorting mechanism in the malaria parasite *Plasmodium falciparum*. *PLoS Pathog* **5:** e1000328.

Richard, D., MacRaild, C.A., Riglar, D.T., Chan, J.A., Foley, M., Baum, J., *et al.* (2010). Interaction between *Plasmodium falciparum* apical membrane antigen 1 and the

rhoptry neck protein complex defines a key step in the erythrocyte invasion process of malaria parasites. *J Biol Chem* **285:** 14815-14822.

Ridley, R.G., Takacs, B., Etlinger, H. and Scaife, J.G. (1990). A rhoptry antigen of *Plasmodium falciparum* is protective in Saimiri monkeys. *Parasitology* **101 Pt 2:** 187-192.

Riglar, D.T., Richard, D., Wilson, D.W., Boyle, M.J., Dekiwadia, C., Turnbull, L., *et al.* (2011). Super-resolution dissection of coordinated events during malaria parasite invasion of the human erythrocyte. *Cell Host Microbe* **9:** 9-20.

Sam-Yellowe, T.Y., Banks, T.L., Fujioka, H., Drazba, J.A. and Yadav, S.P. (2008). *Plasmodium yoelii*: novel rhoptry proteins identified within the body of merozoite rhoptries in rodent *Plasmodium* malaria. *Exp Parasitol* **120:** 113-117.

Sam-Yellowe, T.Y., Florens, L., Wang, T., Raine, J.D., Carucci, D.J., Sinden, R., *et al.* (2004). Proteome analysis of rhoptry-enriched fractions isolated from *Plasmodium* merozoites. *J Proteome Res* **3:** 995-1001.

Sanders, P., Cantin, G., Greenbam, D., Gilson, P., Nebl, T., Moritz, R., *et al.* (2007). Identification of protein complexes in detergent-resistant membranes of *Plasmodium falciparum* schizonts. *Mol. Biochem. Parasitol.* **154:** 148-157.

Schofield, L., Bushell, G.R., Cooper, J.A., Saul, A.J., Upcroft, J.A. and Kidson, C. (1986). A rhoptry antigen of *Plasmodium falciparum* contains conserved and variable epitopes recognized by inhibitory monoclonal antibodies. *Mol Biochem Parasitol* **18:** 183-195.

Soldati, D., Kim, K., Kampmeier, J., Dubremetz, J.F. and Boothroyd, J.C. (1995). Complementation of a *Toxoplasma gondii* ROP1 knock-out mutant using phleomycin selection. *Mol Biochem Parasitol* **74:** 87-97.

Steinfeldt, T., Konen-Waisman, S., Tong, L., Pawlowski, N., Lamkemeyer, T., Sibley, L.D., *et al.* (2010). Phosphorylation of mouse immunity-related GTPase (IRG) resistance proteins is an evasion strategy for virulent *Toxoplasma gondii*. *PLoS Biol* **8:** e1000576.

Stowers, A., Taylor, D., Prescott, N., Cheng, Q., Cooper, J. and Saul, A. (1997). Assessment of the humoral immune response against *Plasmodium falciparum* rhoptry-associated proteins 1 and 2. *Infect-Immun* **65:** 2329-2338.

Topolska, A.E., Lidgett, A., Truman, D., Fujioka, H. and Coppel, R.L. (2004). Characterization of a membrane-associated rhoptry protein of *Plasmodium falciparum*. *J Biol Chem* **279:** 4648-4656.

Trenholme, K.R., Gardiner, D.L., Holt, D.C., Thomas, E.A., Cowman, A.F. and Kemp, D.J. (2000). clag9: A cytoadherence gene in *Plasmodium falciparum* essential for binding of parasitized erythrocytes to CD36. *Proc Natl Acad Sci U S A* **97:** 4029-4033.

Triglia, T., Tham, W.H., Hodder, A. and Cowman, A.F. (2009). Reticulocyte binding protein homologues are key adhesins during erythrocyte invasion by *Plasmodium falciparum*. *Cell Microbiol* **11:** 1671-1687.

Triglia, T., Thompson, J., Caruana, S.R., Delorenzi, M., Speed, T. and Cowman, A.F. (2001). Identification of proteins from *Plasmodium falciparum* that are homologous to reticulocyte binding proteins in *Plasmodium vivax*. *Infect Immun* **69:** 1084-1092.

Waters, A.P., Thomas, A.W., van Dijk, M.R. and Janse, C.J. (1997). Transfection of malaria parasites. *Methods* **13:** 134-147.

Weiss, G.E., Crabb, B.S. and Gilson, P.R. (2016). Overlaying molecular and temporal aspects of malaria parasite invasion. *Trends Parasitol* **32:** 284-295.

Werner, E.B., Taylor, W.R. and Holder, A.A. (1998). A *Plasmodium chabaudi* protein contains a repetitive region with a predicted spectrin-like structure. *Mol-Biochem-Parasitol* **94:** 185-196.

Yamamoto, M. and Takeda, K. (2012). Inhibition of ATF6beta-dependent host adaptive immune response by a *Toxoplasma* virulence factor ROP18. *Virulence* **3:** 77-80.

Yap, A., Azevedo, M.F., Gilson, P.R., Weiss, G.E., O'Neill, M.T., Wilson, D.W., *et al.* (2014). Conditional expression of apical membrane antigen 1 in *Plasmodium falciparum* shows it is required for erythrocyte invasion by merozoites. *Cell Microbiol* **16:** 642-656.

ACKNOWLEDGMENTS

We kindly the Australian Red Cross for red blood cells and serum and Ross Coppel for rhoptry antibodies as well as Scott Chisholm and Paul Gilson for insightful discussions. This work was supported by a grant from the National Health and Medical Research Council (NHMRC) of Australia (Project 1082157). SG is the recipient of a Victorian-Indian Doctoral Scholarship.

FIGURE LEGENDS

Fig. 1. Generation of PbRAP1 and PbRAP2 inducible knockdown parasite lines

A. Schematic representation of the endogenous *RAP1* locus and the *RAP1* locus after integration of the targeting construct. The oligonucleotide primers used to detect 5′ integration (a/b), 3′ integration (c/d) and either the *RAP1* locus (e/f) or *RAP2* locus (g/h) are shown. The K, *Kpn*I; S, *Spe*I restriction enzyme fragments and the region used as a probe for Southern blot analysis are indicated. A similar strategy was used to generate PbRAP2 iKD parasites.

B. Analytical PCR shows the presence of the successful 5′ (5' INT) and 3′ integrant (3' INT) bands at 1.4 Kb and 2.4 kb, respectively for PbRAP1 iKD parasites, and 1.5 Kb and 2.34 Kb, respectively for PbRAP2 iKD parasites, which were absent in wildtype (WT) parasites.

C,D. Southern blot analysis of genomic DNA shows the presence of the expected integrant band (In) in PbRAP1 iKD (C) and PbRAP2 iKD (D) parasites with corresponding loss of a band of an intact *RAP1* locus.

Fig. 2. Expression of RAP1 and RAP2 can be regulated by anhydrotetracycline (ATc)

A,B. Effect of ATc treatment on the *RAP1* (a) and *RAP2* (b) gene expression at the transcriptional level by RT-PCR. Expression of *RAP1* and *RAP2* was knocked down by 3.7- and 2.3-fold, respectively with ATc treatment.

C,D. Immunofluorescence analysis (IFA) confirms the reduction of RAP1 and RAP2 expression in parasites treated with ATc. The fluorescent intensity of labelling in schizonts

(n=100) was quantitated and scored as very low (+), low (++) or similar to wildtype (+++) signals.

Fig. 3. The gross ultrastructure of rhoptries and maturation of merozoites is not affected by depletion of RAP2 but RAP1 knockdown affects RAP2 trafficking

A. Transmission electron microscopy images of PbWT and PbRAP2 iKD merozoites showing normal rhoptry morphology (as depicted by arrowheads). All scale bars are 1 micron.

B. Column graph depicting the number of merozoites formed per mature schizont in the PbRAP1 iKD and PbRAP2 iKD parasite lines in the presence or absence of ATc (n = 50). Error bars represent ± SEM.

C. Schizonts and merozoites labelled with anti-RAP2 antibodies show depletion of RAP1 expression with ATc affects the trafficking of RAP2 to the rhoptries.

D. Schizonts and merozoites labelled with anti-RAP1 antibodies show characteristic punctate labelling typical of rhoptry staining despite the depletion of RAP2 expression.

Fig. 4. RAP1 and RAP2 are not essential for erythrocyte invasion of *P. berghei*.

A. Representative FACS plots showing similar invasion efficiency in both PbRAP1-ATc and PbRAP1+ATc. Parasite DNA is stained with Hoechst while donor erythrocytes are stained with DDAO.

B. Quantitation of invasion rate of PbRAP1 iKD (left panel) and PbRAP2 iKD (right panel) parasites grown in the presence of ATc relative to when grown in the absence of ATc (n=3). Error bars represent ± SEM.

Fig. 5. Depletion of RAP1 or RAP2 in *P. berghei* leads to altered growth phenotypes.

A. Growth curves of RAP1 iKD parasites (left panel) or RAP2 iKD parasites (right panel) in BALB/c mice administered drinking water containing ATc or vehicle control. Each data point represents the mean ± SEM, n = 5 mice per group. *P<0.05; **P<0.01, ***P<0.001 as determined by unpaired t-test.

B. *In vitro* growth analysis of PbRAP1iKD Cycle-II parasites shows a delayed growth phenotype when RAP1 is depleted with ATc, leading to the generation of parasites with abnormal morphology by Giemsa smear and death of ~25% of the parasite population.

Fig. 6. PVM morphology is affected when RAP2 expression is depleted

A,B. PbRAP2 iKD treated with ATc contain ruffled perturbations at the periphery of the parasite, extending into the erythrocyte cytosol. These do not appear to be normal membranous blebs into the erythrocyte as they contain parasite cytosolic material. Arrowheads indicate perturbations to the parasite periphery.

C,D. Parasite protrusions into the host were rarely observed in the PbRAP2 iKD parasites grown in the absence of ATC, or in wild type parasites treated with ATC **(E,F)**, and protrusions in these negative controls were much smaller and less distorted. All scale bars are 1 micron.

Fig. 7. Characterisation of RAP1 in *P. falciparum*

A. IFA with anti-RAP1 antibody at different time points across the parasite cell cycle shows RAP1 persists up to 15 hrs post-invasion. New RAP1 is not synthesized again until schizont stage when the parasites are beginning to segment.

B. Western blot analysis of fractions from solubility assays of erythrocytes infected with *P. falciparum* at the schizont (left panel) and ring stage (right panel). Blots were probed with the antibodies as indicated. SERA5/GAPDH, HSP101 and EXP2 serve as soluble, peripherally-associated membrane proteins and integral membrane protein controls, respectively. Lanes represent soluble proteins after hypotonic lysis, Na_2CO_3-extraction and Triton X-100-extraction. Integral membrane proteins remain in the Triton-X insoluble fraction.

C. Western blot analysis of pelleted tetanolysin-lysed cells incubated in the presence (+) or absence (-) of proteinase K. SBP1, PV1 and GAPDH western blots serve as controls.

Fig. 8. Identification of the RAP1 interactome in ring stages of *P. falciparum*

A. SDS-PAGE gel of material eluted from immunoprecipitations performed using RAP1 or GAPDH antibodies as a control on *P. falciparum* 3D7 lysates from purified ring-stages. The asterisks indicate the regions of the gel that were excised for mass-spectrometry.

B. The total number of peptides of rhoptry proteins and other classes of proteins present in all excised bands.

C. Western blot analysis of immunoprecipitations performed with GAPDH (control) or RAP1 antibodies with the indicated antibodies.

Table 1. Proteins containing a signal sequence or transmembrane domain(s) that affinity purified with RAP1

PlasmoDB Gene ID	Annotation	No. Unique Peptides		SS or TMD
		RAP1	Control	
PF3D7_0917900	Heat shock protein 70 (HSP70-2)	106	15	SS
Pf3D7_1116800	Heat shock protein 101 (HSP101)	83	31	SS
PF3D7_0823800	DNAJ protein, putative	34	8	2-3 TMD
PF3D7_0204100	Conserved *Plasmodium* protein, unknown function	28	0	SS
PF3D7_0827900	Disulphide isomerase (PDI-8)	27	2	SS
PF3D7_1134100	Disulphide isomerase (PDI-11)	18	0	SS
PF3D7_1229100	Multi-drug resistance-associated protein 2 (MRP2)	16	0	10 TMD
Pf3D7_1436300	Translocon component PTEX150 (PTEX150)	13	0	SS
PF3D7_0629500	Amino acid transporter, putative	8	0	9 TMD
Pf3D7_0831700	Heat shock protein HSP70 (HSP70-x)	8	1	SS
PF3D7_1033200	Early transcribed membrane protein 10.2 (ETRAMP10.2)	7	0	SS, TMD
PF3D7_1459400	Conserved *Plasmodium*	7	0	TMD

	protein, unknown function			
Pf3D7_1105600	Translocon component PTEX88 (PTEX88)	7	1	SS

Table 2. Exported proteins that affinity purified with RAP1

PlasmoDB Gene ID	Annotation	No. Unique Peptides	
		RAP1	Control
PF3D7_1108700	Heat shock protein DNAJ homologue (PfJ2)	26	0
PF3D7_0102200	Ring-infected erythrocyte surface antigen (RESA) - contains DNAJ domain	22	1
PF3D7_1149200	Ring-infected erythrocyte surface antigen – contains DNAJ domain	16	0
PF3D7_0703500	Erythrocyte membrane associated antigen	11	0
PF3D7_0424500	Serine/threonine protein kinase FIKK family (FIKK4.1)	9	0
PF3D7_0731300	*Plasmodium* exported protein (PHISTB)	7	0

Figure 1

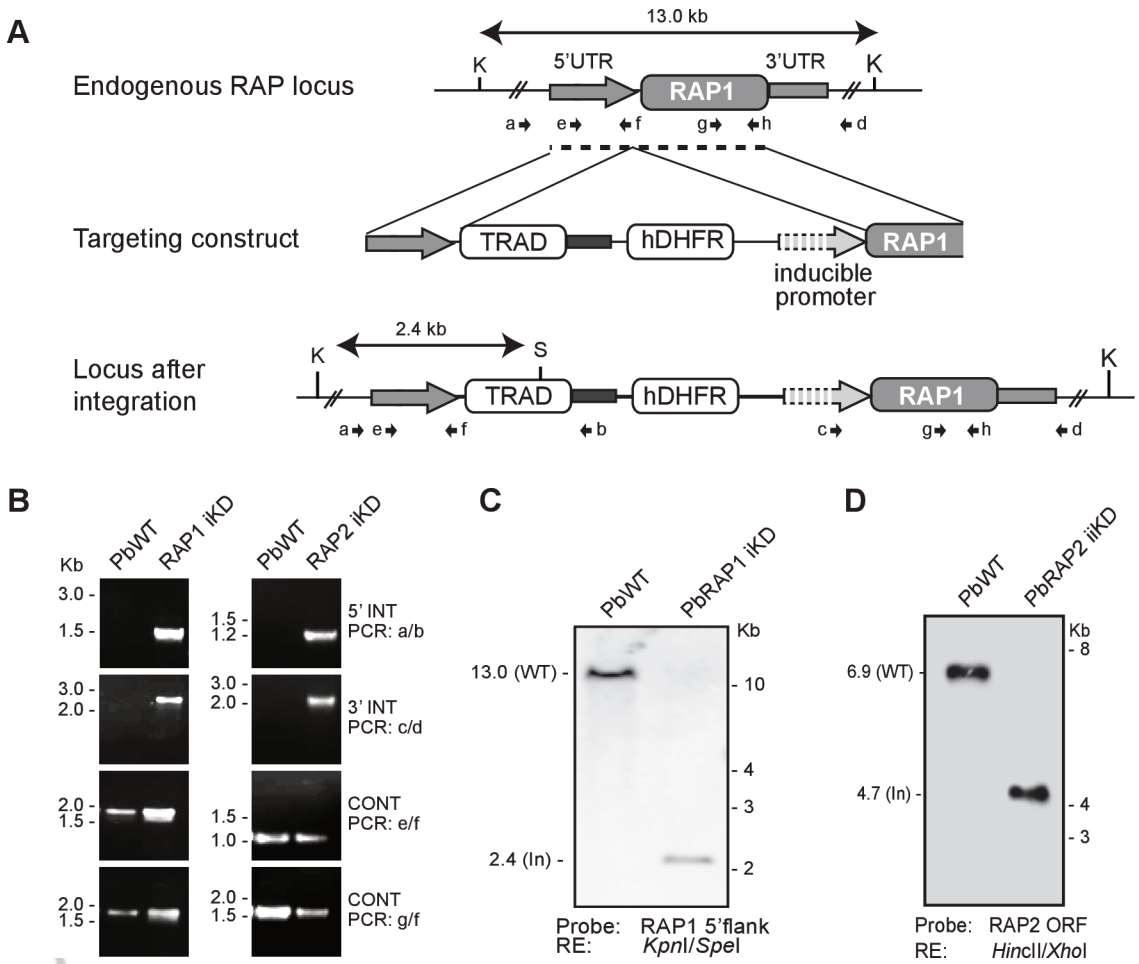

cmi_12733_f1.tif

Figure 2

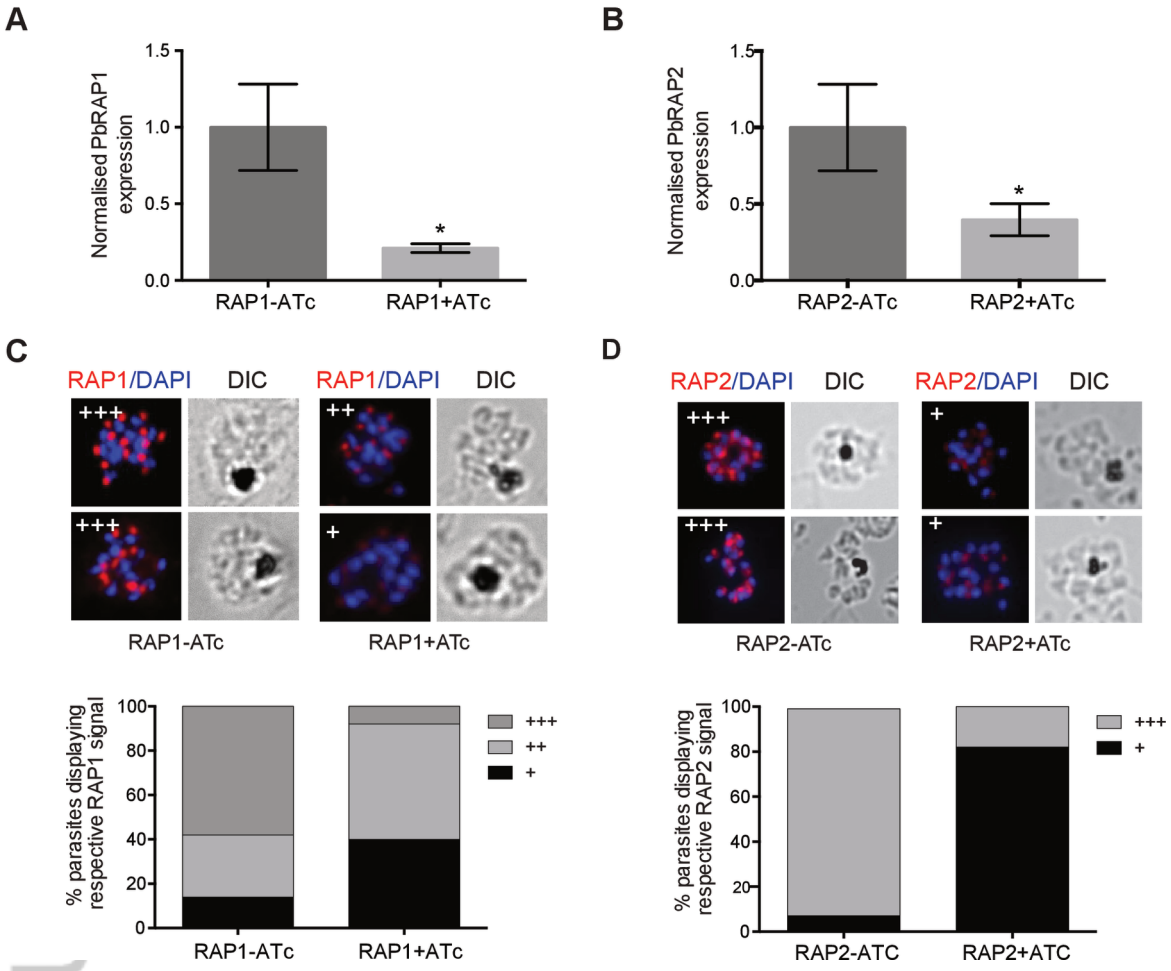

cmi_12733_f2.tif

Figure 1

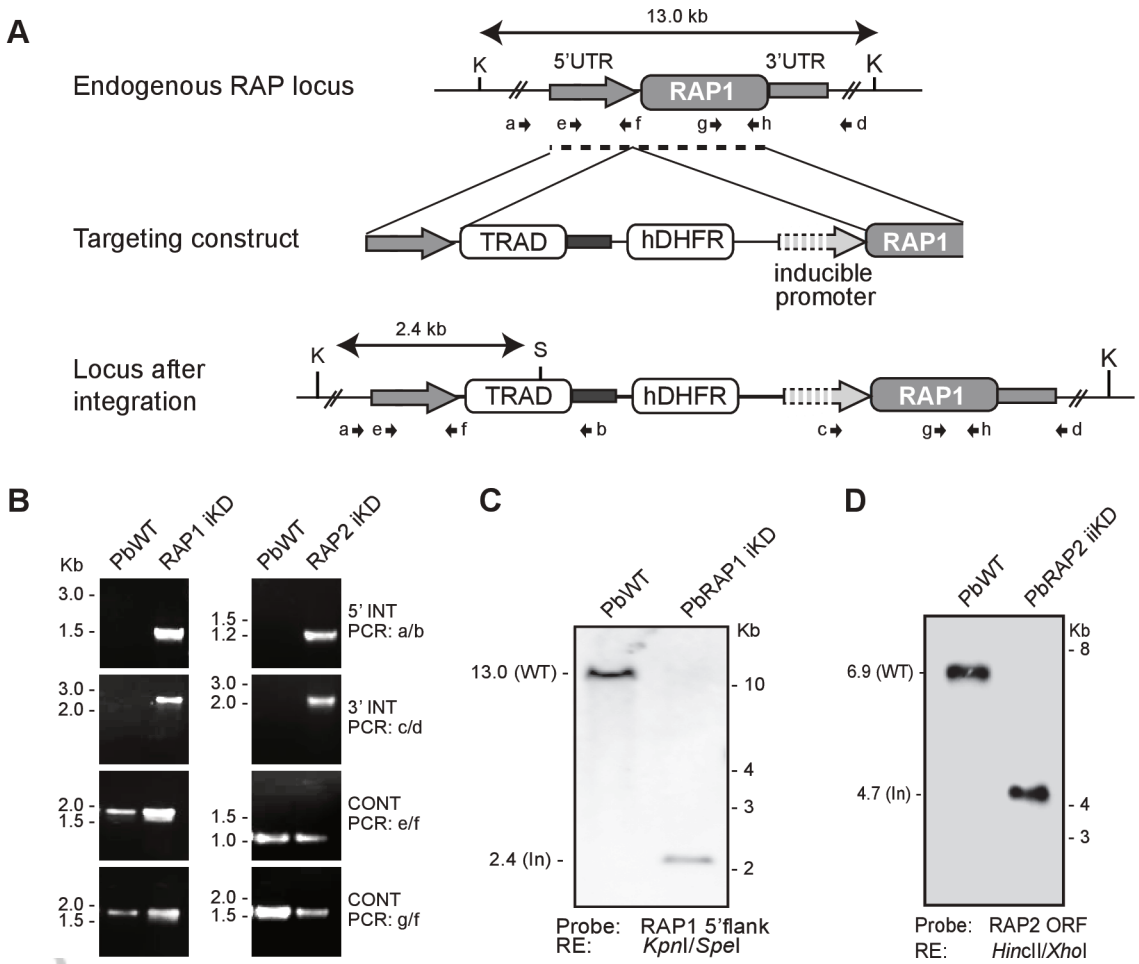

cmi_12733_f1.tif

Figure 2

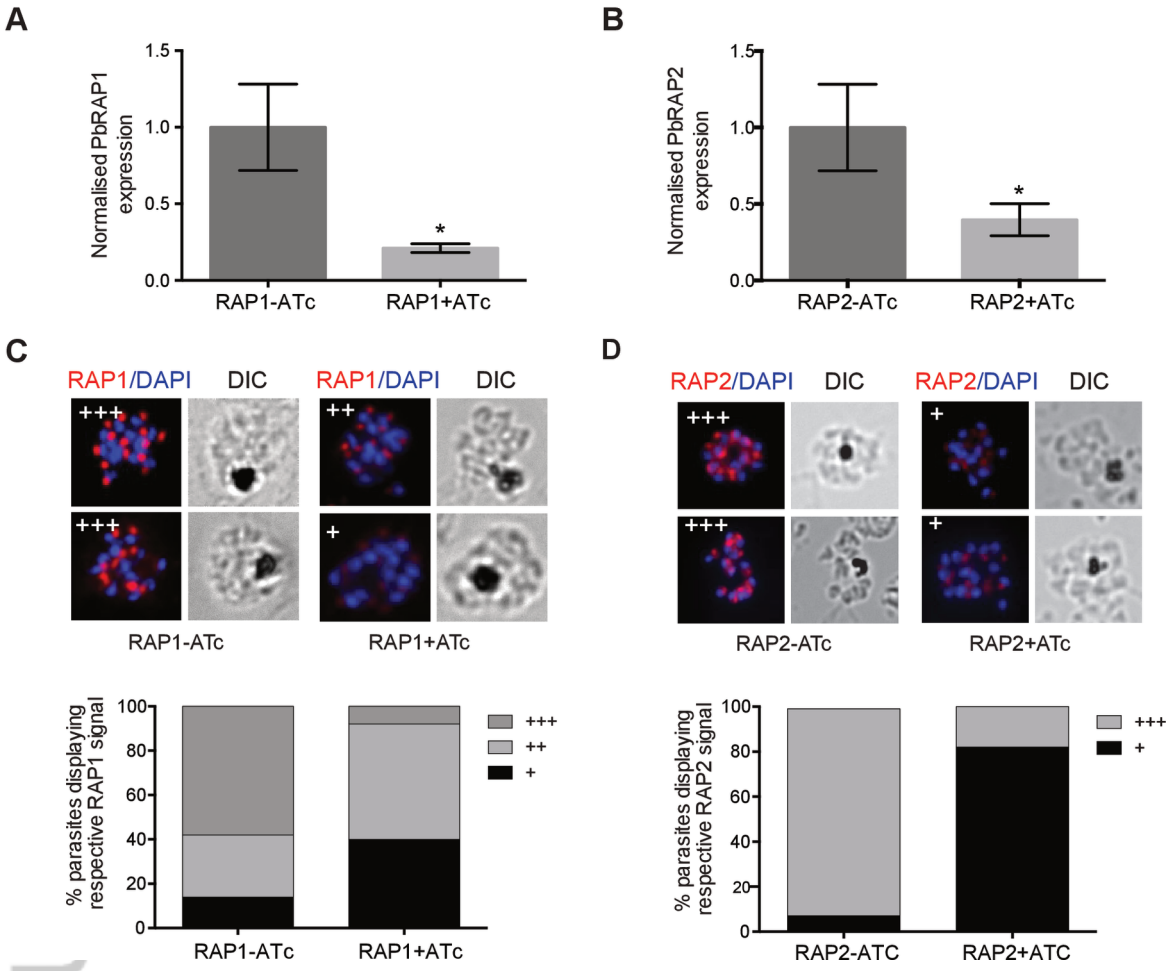

cmi_12733_f2.tif

Figure 3

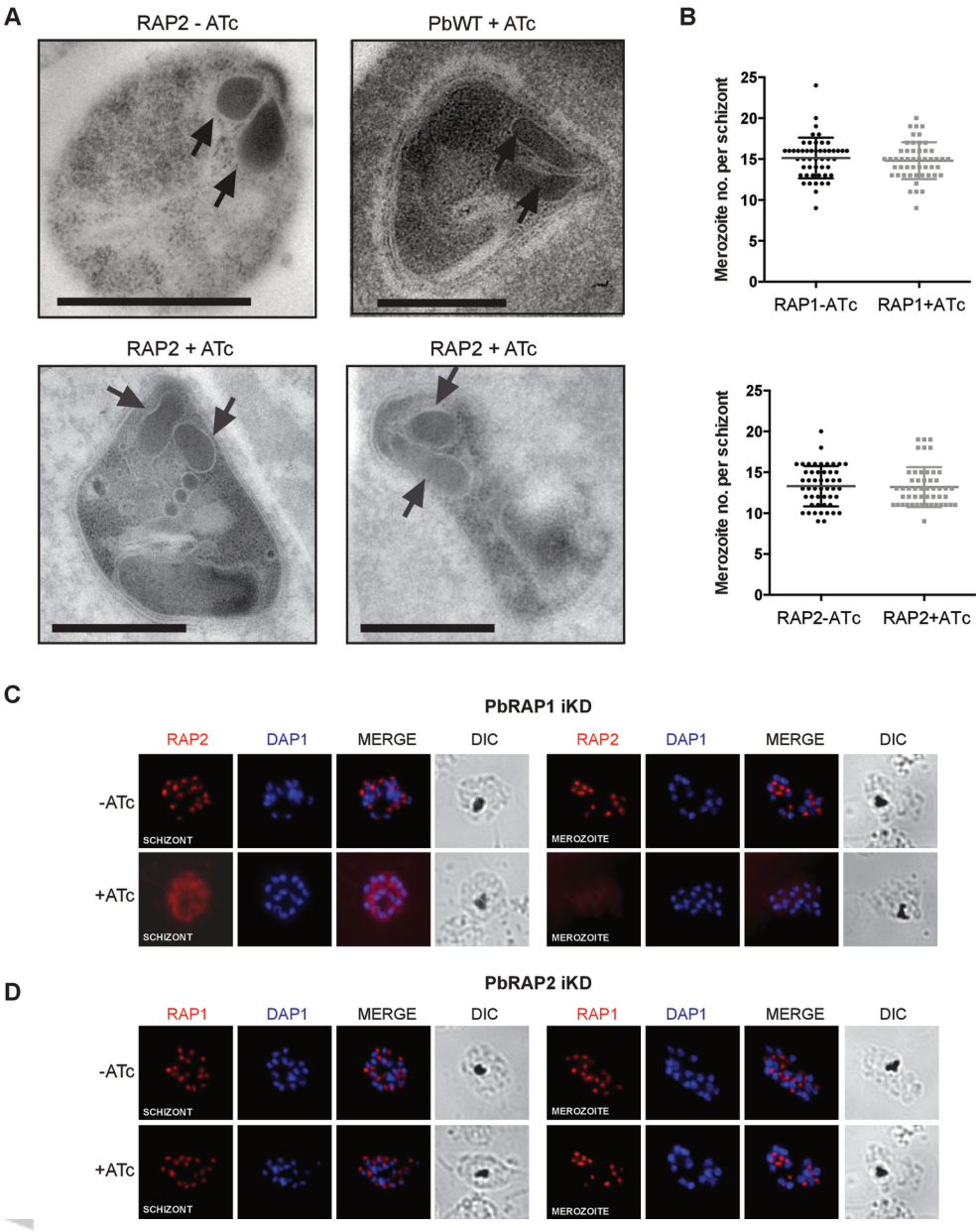

cmi_12733_f3.ai

Figure 4

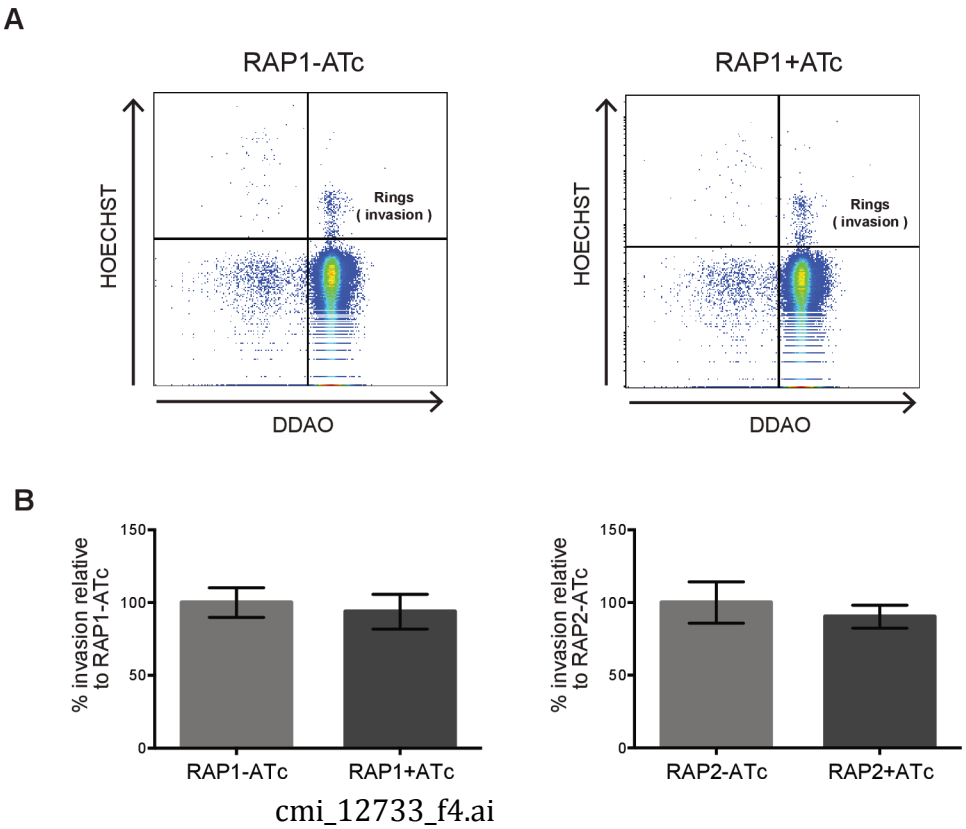

cmi_12733_f4.ai